Engineering Characterization of Bedrock and Design of Rock-Socketed Bored Pile in Eastern Thailand

S. Yimsiri[1], S. Eua-apiwatch[2], and W. Ratananikom[1]*
[1]*Sustainable Civil Engineering and Infrastructure Research Unit, Burapha University, Chonburi, Thailand*
[2]*Department of Civil Engineering, Burapha University, Chonburi, Thailand*
**E-mail*: *wanwarangr@eng.buu.ac.th*

ABSTRACT: This study aims at evaluating and improving design methods of rock-socketed bored piles in Eastern Thailand. The properties of the bedrock at Sriracha district in the Eastern of Thailand are investigated, including physical, index, and engineering properties. Empirical correlations among the obtained index and engineering properties of the bedrock are derived and proposed, which are q_u-$I_{s(50)}$, q_u-H_R, and σ_t-H_R, although the strength of these relationships are quite low. The empirical equations for a rock-socketed bored pile design for the studied area are proposed by verifying them with the dynamic pile load test results. The obtained equations of side and tip resistances are compared with those proposed by various researchers and some comments are also made.

KEYWORDS: Rock-socketed bored pile, Pile capacity, Rock property, Empirical equation, and Dynamic pile load test.

1. INTRODUCTION

A rock-socketed bored pile (also called a drilled shaft) is a common foundation selection when the structure load is relatively large and there is a bedrock at a reasonable depth. The piles are drilled through the soil to the underlying bedrock. These piles can be founded on the surface of the bedrock, or they can be drilled into the bedrock to create rock sockets. The rapid development of the Eastern of Thailand, due to the Eastern Economic Corridor (EEC) Development Plan, has induced construction of high-rise buildings and infrastructures in this area, many of which make use of rock-socketed piles as their foundations. However, there has not been any study on the engineering properties of the bedrock and the relevant design aspects of rock-socketed piles of this area.

This study aims at evaluating and improving design methods of rock-socketed bored piles in Eastern Thailand, which are originally designed on the basis of presumptive values. In this study, the properties of the bedrock at Sriracha district in the Eastern of Thailand are investigated, including physical, index, and engineering properties. Empirical correlations among the obtained index and engineering properties of the bedrock are derived and proposed. Subsequently, the available design procedures for rock-socketed piles are evaluated by verifying their results against the in-situ pile load test data. Finally, the appropriate design procedures for rock-socketed piles in the studied area are proposed.

2. DESIGN OF ROCK-SOCKETED PILE

The ultimate capacity of a rock-socketed pile is a function of many factors including: (i) pile geometry, (ii) strength of rock, (iii) discontinuity of rock mass, (iv) confining stress acting on the pile shaft, (v) interface roughness, and (vi) rock socket cleanliness. It is very complicated to quantify all these aspects in the design; however, it is normal to adopt a simplified assumption of separation of the components of overall ultimate pile capacity to come from side and tip resistances.

2.1 Side Resistance

Based on the conservative approach and local experience, a number of empirical correlations have been published for estimating the rock-socketed side resistance.

2.1.1 Allowable Side Resistance

Table 1 summarizes the published allowable side resistance (f_a) for various rock types. The correlations are based on both intact rock and rock mass properties.

Table 1 Summary of allowable side resistance

Allowable side resistance	Rock types	References
$0.10q_u$	Sandstone	Thorne (1977)
$0.05q_u$	Shale	Thorne (1977)
100 to 1380 kPa	Several	Rowe & Armitage (1984)
300 kPa for RQD<25% 600 kPa for RQD = 25-70% 1000 kPa for RQD>70%	Limestone	Neoh (1998)
500 kPa for grade III rock 1000 kPa for grade II or better rock	Granite	GEO (2006)

Note: q_u = uniaxial compressive strength of intact rock, RQD = rock quality designation

2.1.2 Ultimate Side Resistance Based on Uniaxial Compressive Strength

Empirical correlations between the ultimate side resistance (f_{ult}) and the uniaxial compressive strength of intact rock (q_u) have been proposed by many researchers, the form of which can be generalized as shown in Equation (1). Both linear (B=1) and power (B≠1) equations have been suggested and some of them are summarized in Tables 2 and 3, respectively. For linear relationship, the values of A range from 0.15 to 0.30. For power relationship, the values of A range from 0.20 to 0.45 (smooth socket) and the values of B are typically 0.5.

$$f_{\text{ult}} = Aq_u^B \quad \text{(MPa)} \tag{1}$$

where A and B are empirical factors.

Table 2 Empirical factors for linear side resistance relationship

References	*A*	*B*
Reynolds & Kaderabek (1980)	0.30	1
Gupton & Logan (1984)	0.20	1
Reese & O'Neill (1988)	0.15	1
Toh *et al.* (1989)	0.25	1

2.1.3 Ultimate Side Resistance Based on Additional Rock Mass Parameters

Williams *et al.* (1980) pointed out that the side resistance determined by empirical correlations with q_u does not consider the discontinuities in rock mass and developed the empirical correlation that considers the effect of discontinuities on the side resistance as shown in

Equation (2). The coefficient α is a reduction factor reflecting the strength of the intact rock, i.e. α=f(q_u). The coefficient β is a reduction factor reflecting rock mass effect, i.e. β = f(E_m/E_i), where E_m is the elastic modulus of the rock mass, and E_i is the elastic modulus of the intact rock.

$$f_{\text{ult}} = \alpha\beta q_u \tag{2}$$

O'Neill & Reese (1999) recommended to use a reduction factor (α_E) with Horvath & Kenney (1979)'s equation to account for rock mass behavior as shown in Equation (3), where $\alpha_E = E_m/E_i$.

$$f_{\text{ult}} = 0.2\alpha_E q_u^{0.5} \quad \text{(MPa)} \tag{3}$$

Rezazadeh & Eslami (2017) suggested to modify q_u as shown in Equation (4) to account for the rock mass discontinuities before using empirical correlation in Section 2.1.2. α_E can be estimated from Rock Mass Rating (RMR) and Rock Quality Designation (RQD) as shown in Equations (5) and (6), respectively.

$$q_{um} = \alpha_E^{0.7} q_u \tag{4}$$

$$\alpha_E = 0.1 + \frac{RMR}{1150 - 11.4RMR} \quad (0<\text{RMR}<92) \quad \text{(Kulhawy, 1978)} \tag{5}$$

$$\alpha_E = 10^{0.013RQD - 1.34} \quad \text{(Zhang, 2010)} \tag{6}$$

Table 3 Empirical factors for power side resistance relationship

References	*A*	*B*	Remarks
Rosenberg & Journeaux (1976)	0.38	0.52	
Meigh & Wolski (1979)	0.22	0.60	
Williams *et al.* (1980)	0.44	0.36	
Rezazadeh & Eslami (2017)	0.36	0.36	
Horvath & Kenney (1979)	0.20	0.5	Smooth socket
Horvath & Kenney (1979)	0.30	0.5	Rough socket
Rowe & Armitage (1987)	0.45	0.5	R1, R2, R3 rough sockets
Rowe & Armitage (1987)	0.6	0.5	R4 rough socket
Kulhawy & Phoon (1993)	0.23	0.5	Lower bound
Kulhawy & Phoon (1993)	0.45	0.5	Mean
Kulhawy & Phoon (1993)	0.67	0.5	Rough socket
Zhang & Einstein (1998)	0.4	0.5	Smooth socket
Zhang & Einstein (1998)	0.8	0.5	Rough socket
Ng *et al.* (2001)	0.20	0.5	
Prakoso (2002)	0.32	0.50	

2.2 Tip Resistance

Different methods have been proposed for predicting the tip resistance of rock-socketed piles; however, empirical and semi-empirical correlations have been used most widely.

2.2.1 Allowable Tip Resistance

Table 4 summarizes the published allowable presumptive tip resistance (q_a) for various rock types. It is noted that the ranges given are quite large. Peck *et al.* (1974) suggested an empirical correlation between the allowable tip resistance and RQD. Mehrotra (1992) and GEO (2006) presented allowable tip resistance based on RMR.

Table 4 Summary of allowable tip resistance

Allow. tip resist.	Rock types	References
$2.7q_u$	Theoretical	Rowe & Armitage (1984)
$0.2q_u$	Many building codes	GEO (1991)
150 to >3300 kPa	Various	Krahenbuhl & Wagner (1983)
480 to 9570 kPa	Various	Rowe & Armitage (1984)
3000 to 10000 kPa	Granitic and volcanic	BD (2004)
1000 to 8000 kPa	Various	Zhang (2004)

2.2.2 Ultimate Tip Resistance Based on Uniaxial Compressive Strength

For massive rock (joint spacing > four to five times of pile diameter), the effects of discontinuities are insignificant and intact rock properties can define the ultimate tip resistance. Many attempts have been made to correlate the ultimate tip resistance, q_{ult}, with the uniaxial compressive strength of intact rock, q_u, the form of which can be generalized as shown in Equation (7). Both linear (D=1) and power ($D\neq1$) equations have been suggested and some of them are summarized in Tables 5 and 6, respectively. For linear relationship, the values of C range from 1.0 to 4.5. For power relationship, the values of C range from 3.0 to 6.6 and the values of D are typically 0.5.

$$q_{ult} = C(q_u)^D \quad \text{(MPa)} \tag{7}$$

where C and D are empirical factors.

Table 5 Empirical factors for linear tip resistance relationship

References	*C*	*D*	Remarks
Coates (1967)	3	1	
Rowe & Armitage (1987)	2.7	1	
ARGEMA (1992)	4.5	1	$q_{ult} \leq 10$ MPa
Findlay *et al.* (1997)	1.0 to 4.5	1	

Table 6 Empirical factors for power tip resistance relationship

References	*A*	*B*	Remarks
Vipulanandan *et al.* (2007)	4.66	0.56	
Nam (2004)	2.14	0.66	
Zhang & Einstein (1998)	4.83	0.5	Mean
Zhang & Einstein (1998)	6.6	0.5	Upper bound
Zhang & Einstein (1998)	3.0	0.5	Lower bound
Zhang (2008)	4.93	0.5	

2.2.3 Ultimate Side Resistance Based on Additional Rock Mass Parameters

Relationships have been developed to account for the influence of discontinuities in the rock mass on the tip resistance. For cases in which joint spacing is greater than the socket diameter, failure occurs by splitting which eventually leads to general shear failure, the solution of which is shown in Equation (8) (Kulhawy & Goodman, 1980).

$$q_{ult} = JcN_{cr} \tag{8}$$

where J is a correction factor that depends on normalized spacing of horizontal joints; c is cohesion of rock mass; and N_{cr} is a bearing capacity factor, which is a function of the friction angle of the rock mass (ϕ) and normalized spacing of vertical joints.

For jointed rock mass, when discontinuities are vertical or nearly vertical, and closed joints are present with a spacing less than the socket diameter, a general wedge failure mode may develop and the ultimate tip resistance can be approximated as shown in Equation (9) (NCHRP, 2006).

$$q_{ult} = cN_c s_c + \frac{B}{2}\gamma N_\gamma s_\gamma + \gamma L_p N_q s_q \tag{9}$$

where B is a socket diameter; γ is an effective unit weight of the rock mass; L_p is a pile length; N_c, N_γ, and N_q are bearing capacity factors (depending on ϕ of rock mass); and s_c, s_γ, and s_q are shape factors.

The Canadian Foundation Engineering Manual proposed that the ultimate tip resistance can be calculated using Equation (10) for sedimentary rocks with primary horizontal discontinuities, where discontinuity spacing is at least 0.3 m and discontinuity aperture does not exceed 6 mm (CGS, 1985).

$$q_{ult} = 3q_u K_{sp} D \tag{10}$$

where $K_{sp} = [3+s/B]/[10(1+300g/s)^{0.5}]$ is an empirical factor; s is the spacing of the discontinuities; B is the socket diameter; g is the aperture of the discontinuities; $D=1+0.4(L_s/B)\leq 3.4$ is the depth factor; L_s is the socket length.

The American Association of State Highway and Transportation Officials suggested that the ultimate tip resistance can be estimated using Equation (11) (AASHTO, 1996).

$$q_{ult} = N_{ms} q_u \tag{11}$$

where N_{ms} is an empirical coefficient depending on rock mass quality and rock type.

Zhang (2010) suggested that the uniaxial compressive strength of the rock mass, q_{um}, can be estimated by that of the intact rock, q_u, as shown in Equation (12). The α_E can be estimated from RMR and RQD as shown in Equations (5) and (6), respectively. The relationship between q_{ult} and q_{um} is suggested as shown in Equation (13).

$$q_{um}=(\alpha_E)^{0.7} q_u \tag{12}$$

$$q_{ult} = 6.39(q_{um})^{0.45} \quad \text{(MPa)} \tag{13}$$

For fractured rock, the ultimate tip resistance can be estimated in terms of Hoek-Brown strength parameters as shown in Equation (14) for the case of zero overburden pressure (Carter & Kulhawy, 1988). Zhang & Einstein (1998) derived an expression for the ultimate tip resistance that considers the influence of the overburden stress as shown in Equations (15) and (16).

$$q_{ult} = q_u\left[s^a + (m_b s^a + s)^a\right] \tag{14}$$

$$q_{ult} = A + q_u\left[m_b \frac{A}{q_u} + s\right]^a \tag{15}$$

$$A = \sigma_{v,b}' + q_u\left[m_b \frac{\sigma_{v,b}'}{q_u} + s\right]^a \tag{16}$$

where m_b, s, and a are Hoek-Brown strength parameters for the rock mass which can be estimated empirically using correlation to RMR.

3. SITE AND GEOMATERIAL CHARACTERIZATION

The studied site is at the Queen Srisavarindira Somdej Na Sriracha Hospital in Sriracha district which is located in the eastern gulf coast of Thailand as shown in Figure 1. The topography of the studied area is undulating, rolling, and hilly to mountainous terrain with flat low lands between the mountainous ranges. The land surface slopes gently toward the sea. Two principle rock types, namely (meta)-sedimentary and igneous rocks, are found in the area. More information about the geology of the area can be found in Taiyaqupt *et al.* (1986).

The geotechnical and geological site characterization was performed by 5 exploratory boreholes. Wash boring method was employed to advance the boreholes in the soil layer. The standard penetration test (SPT) was also performed to determine the in-situ soil strength and to collect disturbed soil specimens. A typical soil profile at the site consists of a very stiff to hard sandy clay layer following by a dense sand layer before encountering the bedrock at approximately 20-27 m BGL (below ground level). The groundwater level is 4 m BGL. Rock core drilling was undertaken by a double tube core barrel of NQ-size to obtain rock cores for approximately 5 m BRS (below rock surface). A core size of 47.6 mm in diameter was obtained with a maximum single core-run of 1.0 m in length. The encountered rock type is Quartzite which is nonfoliated metamorphic rock. Figure 2 shows the Rock Quality Designation (RQD), the values of which are between approximately 50-100% corresponds to a rock quality of fair to excellent (Deere, 1968). Figure 3 shows the Rock Mass Rating (RMR), the values of which are between approximately 55-70 corresponds to a classification of rock mass as fair to good (Bieniawski, 1984).

3.1 Physical Properties

Some physical properties of the obtained rock core specimens were determined. Figure 4 shows dry unit weight according to ASTM D6473-15 (it is referred to as bulk specific gravity in this standard), the values of which range between approximately 26.0-26.7 kN/m^3. Figure 5 shows apparent specific gravity (ASTM D6473-15), the values of which range between approximately 2.70-2.77. Figure 6 shows absorption (ASTM D6473-15), the values of which range between approximately 0.3-0.8%. Figure 7 shows porosity (ratio of pore volume to specimen volume), the values of which range between approximately 0.8-2.0%.

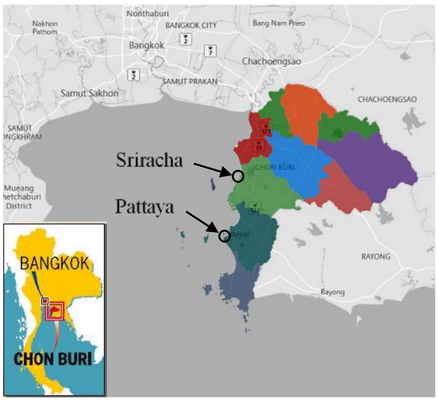

Figure 1 Location of studied areas

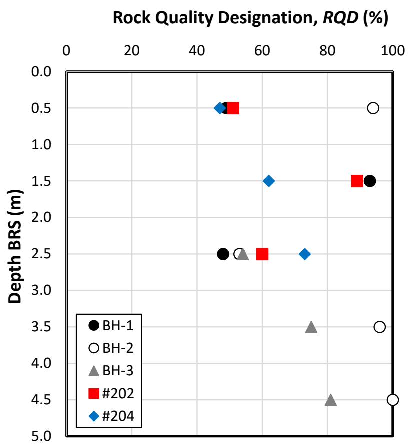

Figure 2 Rock Quality Designation (RQD)

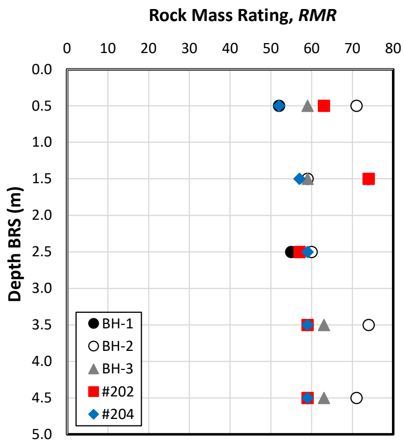

Figure 3 Rock Mass Rating (RMR)

3.2 Uniaxial Compressive Strength

Uniaxial compressive strength (q_u), also commonly termed as unconfined compressive strength, was determined on air-dried intact rock core specimens, which had a diameter of 47.6 mm (NQ size) and a length-to-diameter ratio of 2.0-2.5. The ends of the specimens were made flat and perpendicular to the axis of the specimens. The mean loading rate was chosen about 0.5 MPa/sec in order to confirm the failure time of specimens to ASTM D2938-95 (2-15 min). Figure 8 shows the obtained q_u, the values of which range between approximately 40-80 MPa (excludes outlier data) which can be classified as medium strong to strong rock (ISRM, 1978a).

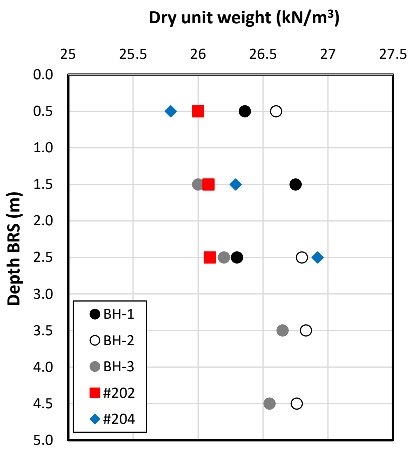

Figure 4 Dry unit weight

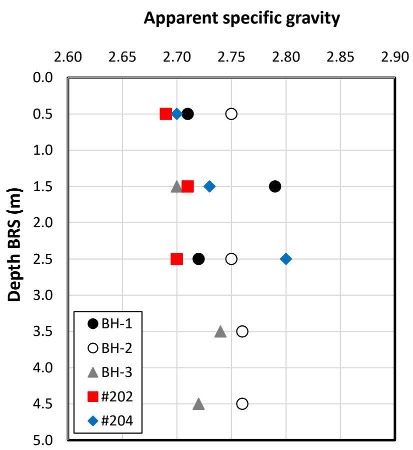

Figure 5 Apparent specific gravity

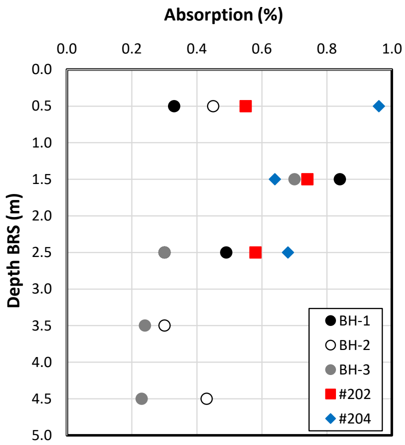

Figure 6 Absorption

3.3 Point Load Strength Index

Point load tests were performed on the cores having a diameter of 47.6 mm (NQ size) and a length-to-diameter ratio of 1.0 (ASTM D5731-16). The tests were carried out on air-dried specimens both in diametral and axial directions. The core being tested is nearly 50 mm in diameter; therefore, the size correction is judged not necessary. The value of the corrected point load strength index ($I_{s(50)}$) is determined by Equation (17). Figure 9 shows the obtained point load strength index, the values of which range approximately between 1.5-3.5 MPa (excludes outlier data) which can be classified as medium strong to strong rock (ISRM, 1978a). The results do not show any anisotropic behavior between diametral and axial tests.

$$I_{s(50)} = P/(D_e)^2 \tag{17}$$

where P= failure load and D_e = equivalent core diameter.

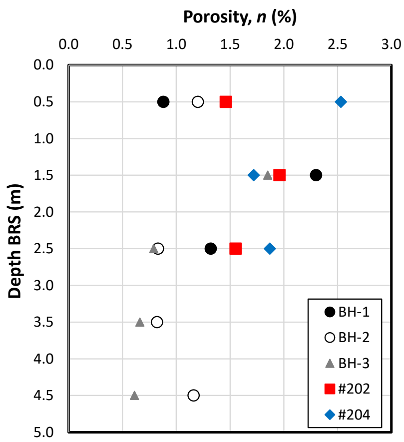

Figure 7 Porosity

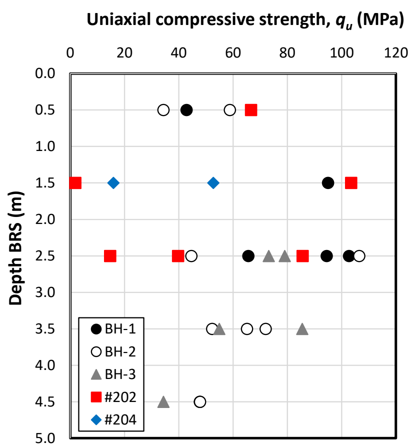

Figure 8 Uniaxial compressive strength

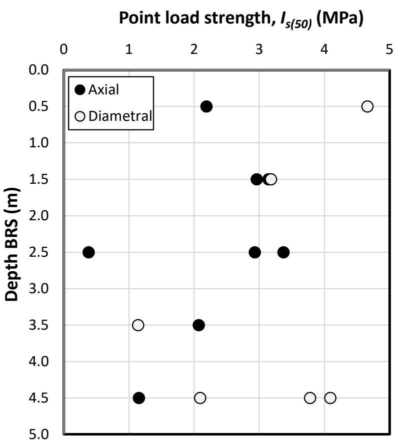

Figure 9 Point load strength index

3.4 Splitting Tensile Strength

Splitting tensile strength (σ_t), also commonly termed as Brazilian tensile strength, was determined on air-dried intact rock core specimens, which had a diameter of 47.6 mm and a thickness-to-diameter ratio of 0.2-0.75 (ASTM D3967-16). The σ_t values were obtained by Equation (18). Figure 10 shows the splitting tensile strength, the values of which ranges approximately between 4.0-9.0 MPa (excludes outlier data).

$$\sigma_t = 2P/(\pi Dt) \tag{18}$$

where P = failure load, D and t are the diameter and thickness of the rock specimen, respectively.

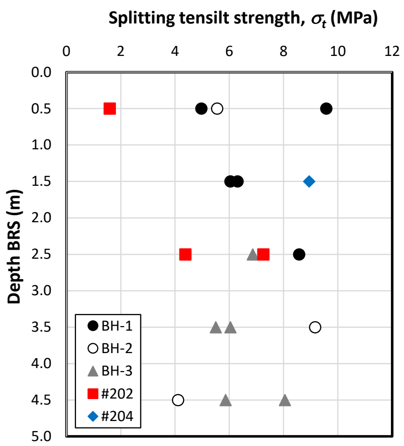

Figure 10 Splitting tensile strength

3.5 Schmidt Hammer

Schmidt hammer rebound tests were performed by an N-type hammer, having impact energy of 2.207 N-m, in accordance with ASTM D5873-14, on air-dried specimens of NQ size (diameter 45.7 mm). In order to avoid orientation corrections, the hammer was held vertically downward at right angles to the horizontal faces of the cylindrical cores in a V-block having a weight of approximately 20 kg. To obtain the average Schmidt hammer rebound number, at least one plunger diameter distance was kept between impacts and 10 single readings were taken on each rock specimen. Then, rebound numbers diverting more than 7 units from the average were discarded and the remaining numbers were averaged again. Figure 11 shows rebound hardness number, the values of which ranges between approximately 40-50 which can be classified as strong rock (ISRM, 1978b).

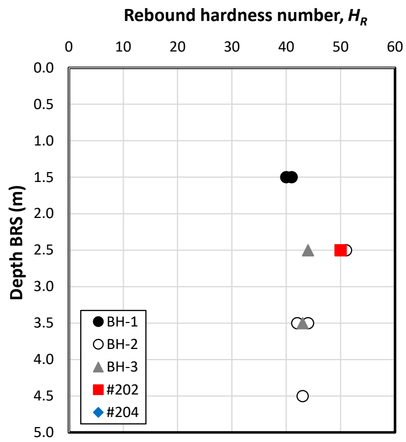

Figure 11 Rebound hardness number

3.6 P-Wave Velocity

The P-wave velocity (V_p) was measured on air-dried specimens by pulse transmission technique, using a Portable Ultrasonic Non-destructive Digital Indicating Tester (PUNDIT). The longitudinal velocities were measured along the length of cored samples. The length of the specimens was determined within an accuracy of 0.1 mm and the time of ultrasonic pulse was read with an accuracy of 0.1 μs. The V_p can be obtained by dividing the core length by the measured travel time according to Equation (19). Figure 12 shows P-wave velocity, the values of which are approximately 6,000 m/s (excluding outlier data).

$$V_p = L/t \tag{19}$$

where V_p = P-wave velocity, t = transition time of wave, L = length of sample

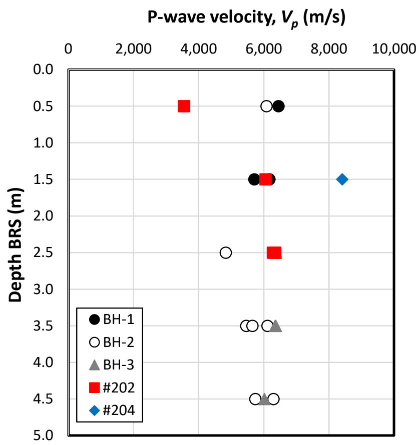

Figure 12 P-wave velocity

3.7 Young's Modulus

The Young's modulus (E) was obtained from the slope of the initial linear portion of the stress-strain curve. The axial strain was measured using a dial gage with precision of 0.01 mm. Figure 13 shows Young's modulus, the values of which ranges between approximately 10-20 GPa (excluding outlier data). Figure 14 shows the relationship between E and q_u which gives ratios of between approximately 180-350 (excluding outlier data) which can be classified as medium modulus ratio (Deere & Miller, 1966).

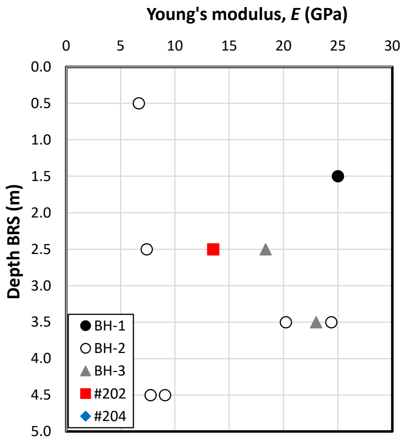

Figure 13 Young's modulus

3.8 Empirical Correlations

Simple linear regression analyses with zero intercept was conducted to examine relationships between various rock properties investigated earlier. The data of granite at nearby Pattaya site (Khao Pra Tum nak) are also included, the location of which is shown in Figure 1. In general, the relationship among investigated rock properties cannot be observed. Nonetheless, there are positive relations between 3 pairs of parameters, i.e. q_u-$I_{s(50)}$ (Figure 15), q_u-H_R (Figure 16), and σ_t-H_R (Figure 17), although the strength of these relationships are quite low. Equation (20) shows an obtained relationship between q_u-$I_{s(50)}$. The obtained conversion factor (K) of 16.501 is consistent with those reported by, e.g. Ghosh & Srivastava (1991) and Kohno & Maeda (2012). It is also comparable with other published data which were reviewed by e.g. Kahraman (2014) and Tandon & Gupta (2015), although it is less than general number of 23-24 (ASTM D5731-16). Equation (21) shows an obtained relationship between q_u-H_R which is consistent with that of Singh *et al.* (1983) and is also comparable with other published data which were reviewed by e.g. Selcuk & Yabalak (2015) and Rahimi *et al.* (2022). Equation (22) shows an obtained relationship between σ_t-H_R which is comparable with those of Kilic & Teymen (2008) and Jamshidi *et al.* (2018) as also shown in Figure 17. It is also found that the ratios of q_u/σ_t have an average value of 14.1 which is comparable with that of Altindag & Guney (2010) but higher than those of Kahraman *et al.* (2012) and Nazir *et al.* (2013).

$$q_u = 16.501 I_{s(50)} \tag{20}$$

$$q_u = 1.830 H_R \quad \text{(MPa)} \tag{21}$$

$$\sigma_t = 0.146 H_R \quad \text{(MPa)} \tag{22}$$

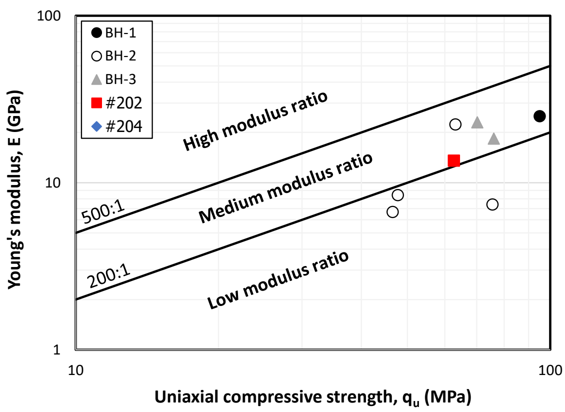

Figure 14 Modulus ratio (after Deere & Miller, 1966)

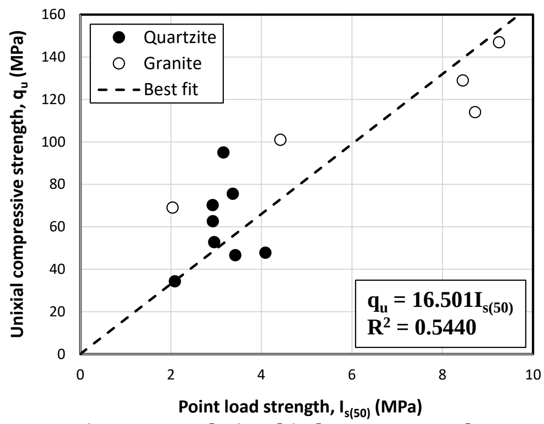

Figure 15 Relationship between q_u and $I_{s(50)}$

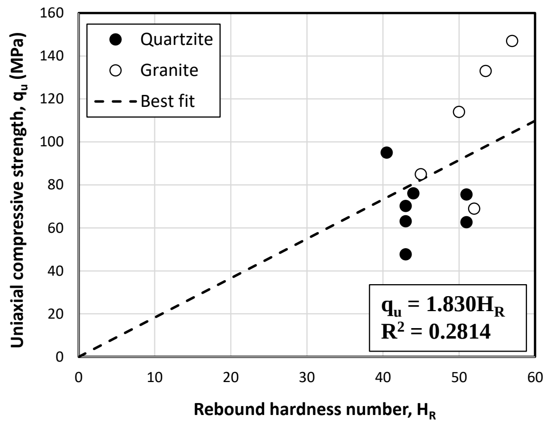

Figure 16 Relationship between q_u and H_R

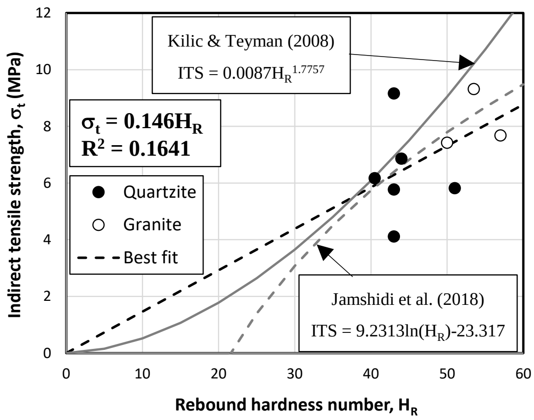

Figure 17 Relationship between σ_t and H_R

4. IN-SITU TESTING OF PILES

Rock-socketed bored piles with a diameter of 1.5 m were constructed as a foundation of a 26-stories building in the studied area. The piles were constructed by wet process, with bentonite as a stabilizing liquid, through soil and socketed into the bedrock with a length of 1.0 m BRS. The rock sockets were constructed by chiseling by mechanical impact. The dynamic pile load tests were performed on 4 piles, the soil conditions of which are shown in Figures 18 to 21. The soil properties are interpreted based on SPT data. In clay, the undrained shear strength (s_u) is estimated by correlation of Stroud (1974) as shown in Equation (23). In sand, the friction angle (ϕ') is estimated by correlation of Peck *et al.* (1974) as shown in Equation (24) by using corrected SPT for overburden pressure proposed by Skempton (1986) as shown in Equation (25).

$$s_u\ (\text{kPa}) = 4.4N_f \tag{23}$$

$$\phi'(\text{degree}) = 27.1+0.3N_1-0.0054N_1^2 \tag{24}$$

$$N_1 = C_N N_f \quad \text{where} \quad C_N = \frac{2}{1+\frac{\sigma_v'(\text{kPa})}{100}} \tag{25}$$

where N_f = SPT obtained from field, N_1 = corrected SPT, and C_N = correction factor

The results of dynamic pile load test (DPLT) are summarized in Table 7. The tests were performed by a 20-ton hammer with a raise distance of 1.8 m. The tests were done between 100-300 days after pile construction. The DPLT results by CAPWAP provide direct measurement of ultimate side and tip resistances of the piles against which analytical models can be evaluated. To obtain the side resistance of the rock socket, the side resistance of soil is subtracted from the total side resistance obtained from DPLT. The side resistance of clay is calculated by α method (Equation (26)), where α is a function of s_u as suggested by Kulhawy & Jackson (1989). The side resistance of sand is calculated by Equation (27), where K = 1-sin ϕ' and $\delta = 0.8\phi'$. The critical depth for calculating side resistance in sand is taken as 15D, where D = pile diameter (Das, 2016).

The values of side resistance of each soil layer are presented in Figures 18 to 21.

$$f_s = \alpha s_u \tag{26}$$

$$f_s = K\sigma_v'\tan\delta \tag{27}$$

There are 3 piles with their length of more than 20 m (#59, #382, and #435) and 1 pile with the length of 10 m (#231). Before being tested, Pile #231 was cut (from its original length of 20 m) after the excavation of the basement. It is noted that the tip resistance component of the pile capacity will be mobilized only after significant displacements have occurred, at loads large enough to cause slip along the full length of the pile. This may not be the case for the DPLT results of Piles #59, #382, and #435 which give lower ultimate tip resistance because it still cannot be fully mobilized due to their large pile length. In contrast, the DPLT results of Pile #231 show larger ultimate tip resistance because it can be more mobilized due to its smaller pile length. This assumption is validated by the observed pile movements during DPLT. Consequently, the DPLT results of Piles #59, #382, and #435 are used for side resistance verification, whereas the DPLT results of Piles #231 are used for tip resistance verification.

Table 7 Dynamic pile load test results

Pile No.	#59	#382	#435	#231	Remarks
Length (m)	27	26	20	10	Pile #231 was cut and tested after basement excavation.
Ultimate side resistance (kN)	15329	14471	13074	3494	From DPLT
Ultimate tip resistance (kN)	8453	7396	7392	13960	From DPLT
Ultimate side resistance (soil) (kN)	5744	5443	4585	1588	Details shown in Figs. 19-21
Ultimate side resistance (rock) (kN)	9585	9028	8489	1906	
Ultimate side resistance (rock) (kPa)	2034	1916	1801	404	1.0 m socket length
Ultimate tip resistance (rock) (kPa)	4783	4185	4183	7900	
Allowable side resistance (rock) (kPa)	814	766	721	162	FS = 2.5
Allowable tip resistance (rock) (kPa)	1913	1674	1673	3160	FS = 2.5
Uniaxial compressive strength, q_u (MPa)	80	54	59	66	Average of 5 m BRS
RQD	63	64	86	76	Average of 5 m BRS
RMR	60	60	67	63	Average of 5 m BRS

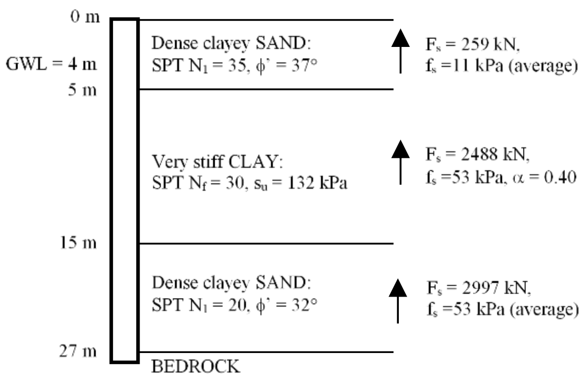

Figure 18 Soil condition at Pile #59

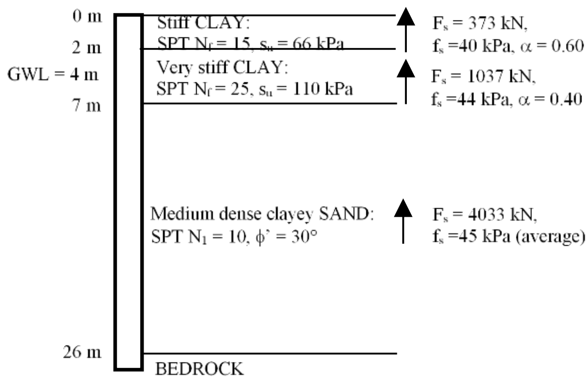

Figure 19 Soil condition at Pile #382

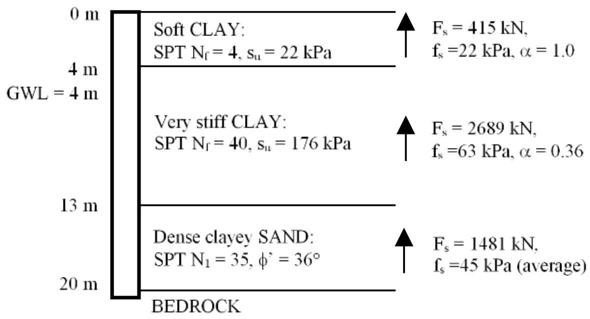

Figure 20 Soil condition at Pile #435

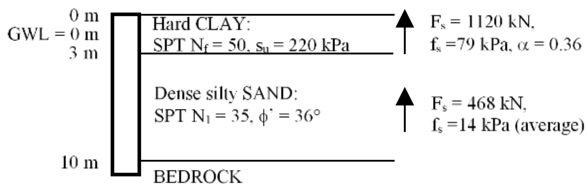

Figure 21 Soil condition at Pile #231

5. VERIFICATION AGAINST DPLT RESULTS

Generally, the design of foundations requires performance check to satisfy both ULS and SLS criteria. However, the design of bored piles socketed into rock is normally governed by displacement considerations. Nevertheless, the ultimate capacity of the pile must always be evaluated to determine the degree of safety of the proposed design. Moreover, a factor-of-safety approach can often be adopted in an attempt to control SLS requirements implicitly through a ULS concept.

5.1 Side Resistance

Table 8 shows the obtained allowable side resistance with a Factor of Safety (FS) of 2.5. The average allowable side resistance is 767 kPa which is consistent with those suggested by Neoh (1998) and GEO (2006). The obtained correlation between f_a and q_u is shown in Equation (28) which is much smaller than that suggested by Thorne (1977) (see Table 1).

$$f_a = 0.012q_u \tag{28}$$

Table 8 Allowable side resistance

Description	#59	#382	#435	Remarks
Allow. side resist. (kPa)	814	766	721	From Table 7
f_a/q_u	0.010	0.014	0.012	Average = 0.012

Table 9 shows the obtained ultimate side resistance, the average of which is 1917 kPa. The obtained linear and power relations between q_{ult} and q_u are shown in Equations (29) and (30), respectively. The coefficient *A* of the obtained linear relation (0.030) is lower than those reported by various researchers (see Table 2). The coefficient *A* of the obtained power relation (0.241) is consistent with those reported by Kulhawy & Phoon (1993) (lower bound) (see Table 3). The f_{ult} by Williams *et al.* (1980) overestimates the DPLT results, whereas the results of O'Neill & Reese (1999)'s method much underestimate the DPLT results. Equations (33) and (34) show the linear and power relation according to Rezazadech & Eslami (2017), where α_E is estimated from RMR (Equation (5)). Equations (35) and (36) show the linear and power relation according to Rezazadech & Eslami (2017), where α_E is estimated from RQD (Equation (6)).

Figure 22 shows the comparison of the calculated and measured side resistance which also give a degree of scatter of the estimation. It can be seen that the results from power relations (Equations (30), (34), and (36)) give less scatter approximation than those from linear relation (Equations (33), and (35)). Due to the ease of use, Equations (30) and (36) are recommended for estimating the ultimate side resistance.

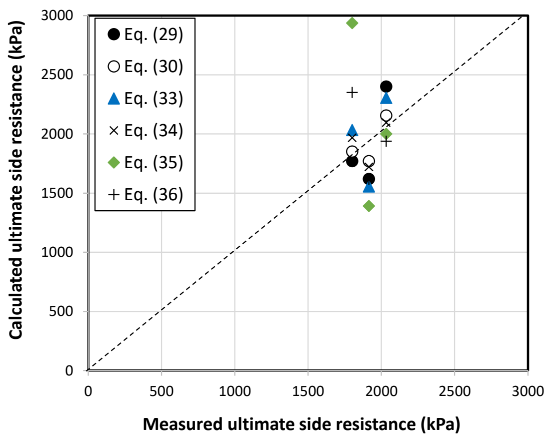

Figure 22 Comparison of calculated and measured side resistance

Table 9 Ultimate side resistance (unit: kPa)

Eq. #	Description	#59	#382	#435	Remarks
	Ultimate side resistance	2034	1916	1801	From Table 7
29	$f_{ult} = 0.030q_u$	2400	1620	1770	Eq. (1)
30	$f_{ult} = 0.241q_u^{0.5}$	2156	1771	1851	Eq. (1)
31	Williams *et al.* (1980)	4288	3256	3717	Eq. (2)
32	O'Neill & Reese (1999)	409	336	420	Eq. (3)
33	$f_{ult} = 0.126q_{um}$	2306	1556	2033	Use RMR, Eqs. (4) & (5)
34	$f_{ult} = 0.490q_{um}^{0.5}$	2096	1722	1968	Use RMR, Eqs. (4) & (5)
35	$f_{ult} = 0.083q_{um}$	2001	1391	2937	Use RQD, Eqs. (4) & (6)
36	$f_{ult} = 0.395q_{um}^{0.5}$	1939	1617	2350	Use RQD, Eqs. (4) & (6)

Notes: 1. Williams *et al.* (1980): $\alpha = f(q_u)$ which is approximately 0.08 to 0.09. $\beta = f(\alpha_E)$ which is approximately 0.67 to 0.70 and α_E is approximated from RMR as shown in Equation (5).

2. O'Neill & Reese (1999): α_E is approximately 0.23 to 0.27 which is estimated from RMR as shown in Equation (5).

In this study, α_E estimated from RMR (Equation (5)) is between 0.23 and 0.27, whereas α_E estimated from RQD (Equation (6)) is between 0.30 and 0.60.

5.2 Tip Resistance

Table 10 shows the obtained allowable tip resistance with a Factor of Safety (FS) of 2.5 which is within ranges suggested by various researchers (see Table 4). The obtained allowable tip resistance corresponds to that suggested by Mehrotra (1992); however, it is much lower than those suggested by Peck *et al.* (1974) and GEO (2006). The obtained correlation between q_a and q_u is shown in Equation (37) which is also smaller than those suggested by GEO (1991) and Rowe & Armitage (1984).

$$q_a = 0.048q_u \tag{37}$$

Table 10 Allowable tip resistance

Description	#231	Remarks
Allowable tip resistance (kPa)	3160	From Table 7
q_a/q_u	0.048	
q_a (kPa) from RQD	12000	Peck et al. (1974)
q_a (kPa) from RMR	2800	Mehrotra (1992)
q_a (kPa) from RMR	7500	GEO (2006)

Table 11 shows the obtained ultimate tip resistance. The obtained linear and power relations between q_{ult} and q_u are shown in Equations (38) and (39), respectively. The obtained coefficient *A* of the linear relation (0.120) is much lower than those reported by various researchers (see Table 5). The obtained coefficient *A* of the power relation (0.972) is also much lower than those reported by many researchers (see Table 6). The q_{ult} by general wedge failure gives somewhat overestimation, whereas Kulhawy & Goodman (1980)'s method gives larger overestimation. Besides, other methods give very large overestimation of q_{ult}. Due to the ease of use, Equation (39) is recommended for estimating the ultimate tip resistance.

Table 11 Ultimate tip resistance (unit: kPa)

Eq. #	Description	#231	Remarks
	Ultimate tip resistance	7900	From Table 7
38	$q_{\text{ult}} = 0.120q_u$	7920	Eq. (7)
39	$q_{ult} = 0.972q_u^{0.5}$	7897	Eq. (7)
40	Kulhawy & Goodman (1980)	11088	Eq. (8)
41	General wedge failure	8339	Eq. (9)
42	CGS (1985)	29702	Eq. (10)
43	AASHTO (1989)	25080	Eq. (11)
44	Zhang (2010)	27064	From RMR, Eqs. (12) & (13)
45	Zhang & Einstein (1998)	57341	Eqs. (15) & (16)

Notes:
1. Kulhawy & Goodman (1980): *J* is 0.42, which is estimated from spacing of horizontal crack (*H*) and pile diameter (*B*). N_{cr} is 4, which is estimated from spacing of vertical crack (*s*) and pile diameter (*B*). The fracture frequency is estimated between 2 and 7 per meter from RQD (Farmer, 1983). Cohesion is estimated as $0.1q_u$ and ϕ is estimated as 30° from RQD (Kulhawy & Goodman, 1980).
2. General wedge failure: Cohesion is estimated as 300 kPa from RMR (Waltham, 1994). ϕ is estimated as 30° from RQD (Kulhawy & Goodman, 1980).
3. CGS (1985): K_{sp} is 0.12 by using the fracture frequency of between 2 and 7 per meter estimated from RQD (Farmer, 1983) and g/s = 0.02.
4. AASHTO (1989): N_{ms} is 0.38, which is estimated from rock category C and RMR/RQD (Zhang, 2004).
5. Zhang (2010): q_{um} is estimated from RMR (Eq. (5)).
6. Zhang & Einstein (1998): a=0.5, s=0.004, and m_b=1.5 estimated from rock category C and RMR/RQD (Carter & Kulhawy, 1988).

6. CONCLUSIONS

In this study, the properties of the bedrock at Sriracha district in the Eastern of Thailand are investigated, including physical, index, and engineering properties. Table 12 summarizes the obtained properties of intact rock and rock mass from 5 m BRS. Moreover, there are empirical relations among obtained rock properties that can be proposed, i.e. q_u-$I_{s(50)}$ (Equation (20)), q_u-H_R (Equation (21)), and σ_t-H_R (Equation (22)), although the strength of these relationships are quite low.

Table 12 Summary of rock properties at Sriracha

Properties	Values	Remarks
Dry unit weight (kN/m^3)	26.0-26.7	
Apparent specific gravity	2.70-2.77	
Absorption (%)	0.3-0.8	
Porosity (%)	0.8-2.0	
Uniaxial compressive strength, q_u (MPa)	40-80	medium strong to strong
Point load strength index, $I_{s(50)}$ (MPa)	1.5-3.5	medium strong to strong
Splitting tensile strength, σ_t (MPa)	4.0-9.0	
Rebound hardness number, H_R	40-50	
P-wave velocity, V_p (m/s)	6000	
Young's modulus, *E* (GPa)	10-20	
E/q_u	180-350	medium modulus ratio
Rock Quality Designation (RQD) (%)	50-100	fair to excellent
Rock Mass Rating (RMR)	55-70	fair to good

The empirical correlations for a rock-socketed pile design for the studied area are proposed by verifying them with the dynamic pile load test results, the summary of which is presented in Table 13. The obtained allowable and ultimate side resistances are consistent with those proposed by other researchers; however, the obtained allowable and ultimate tip resistances are much lower than others. This may be due to the fact that the ultimate tip resistance from DPLT has not been fully mobilized. It is noted that the population of the analyzed correlated data is relatively limited in this study. Therefore, the predicted outcome of the proposed equations could be used at the preliminary stage of designing a structures in this area. Additional results of static pile load tests to failure will help improving the accuracy of the proposed empirical correlation, especially for tip resistance.

Table 13 Proposed empirical correlations

Values	Proposed empirical correla.	Remarks
Allowable side resistance (f_a)	700 kPa	
Ultimate side resistance (f_{ult})	$f_{\text{ult}} = 0.241q_u^{0.5}$ (MPa)	Consistent with Kulhawy & Phoon (1993) (Lower bound)
	$f_{\text{ult}} = 0.395q_{um}^{0.5}$ (MPa)	Rezazadech & Eslami (2017). α_E is estimated from RQD (Eq. (6)).
Allowable tip resistance (q_a)	3000 kPa	
Ultimate tip resistance (q_{ult})	$q_{ult} = 0.972q_u^{0.5}$ (MPa)	

7. ACKNOWLEDGEMENTS

This work is supported by Burapha University and Thailand Science Research and Innovation (TSRI) (Grant #65/2565) and by the Research and Development Fund of Burapha University to the Sustainable Civil Engineering and Infrastructure Research Unit (Grant #12/2565). Mr. Saharat Weerakijphanich, Mr. Kanchit Sisat, Mr. Jakkrit Hattawijit, and Mr. Anuwat Lamlerd provided some help on performing laboratory experiments. Pile load test data were supplied by Italthai Trevi Co., Ltd.

8. REFERENCES

AASHTO (1996). "Standard Specifications for Highway Bridges." *16th Ed., American Association of State Highway and Transportation Officials, Washington, D.C., USA.*

Altindag, R. and Guney, A. (2010). "Predicting the Relationships Between Brittleness and Mechanical Properties (UCS, TS And SH) of Rocks." *Scientific Research and Essays*, 5(16), 2107–2118.

ARGEMA (1992). "Design Guides for Offshore Structures: Offshore Pile Design." *Ed. Tirant, E´ ditions Technip, Paris, France.*

ASTM D2938-95 (2017). "Standard Test Method for Unconfined Compressive Strength of Intact Rock Core Specimens (Withdrawn)." *ASTM International, West Conshohocken, PA, USA.*

ASTM D3967-16 (2016). "Standard Test Method for Splitting Tensile Strength of Intact Rock Core Specimens." *ASTM International, West Conshohocken, PA, USA.*

ASTM D5731-16 (2017). "Standard Test Method for Determination of The Point Load Strength Index of Rock and Application to Rock Strength Classifications." *ASTM International, West Conshohocken, PA, USA.*

ASTM D5873-14 (2016). "Standard Test Method for Determination of Rock Hardness by Rebound Hammer Method." *ASTM International, West Conshohocken, PA, USA.*

ASTM D6473-15 (2018). "Standard Test Method for Specific Gravity and Absorption of Rock for Erosion Control." *ASTM International, West Conshohocken, PA, USA.*

BD (2004). "Code of Practice for Foundations." *Buildings Department, Hong Kong.*

Bieniawski, Z. T. (1984). "Rock Mechanics Design in Mining and Tunneling." *Balkema, Rotterdam.*

Canadian Geotechnical Society (CGS) (2006). "Canadian Foundation Engineering Manual." *4th Ed.*

Carter, J. P., and Kulhawy, F. H. (1988). "Analysis and Design of Drilled Shaft Foundations Socketed into Rock." EPRI EL-5918

Coates, D. F. (1967). "Rock Mechanics Principles." *Queen's Printer.*

Das, B. M. (2016). "Principles of Foundation Engineering." *8th Ed., Cengage Learning.*

Deere, D. U. (1968). "Geological considerations. Rock Mech. in Engg. Practice." *Eds. Stagg & Zienkiewicz,* 1-20.

Deere, D. U. and Miller, R. P. (1966). "Engineering Classification and Index Properties for Intact Rocks." *Tech. Report, Air Force Weapons Lab, No. AFNL-TR,* 65–116.

Farmer, I. W. (1983). "Engineering Behaviour of Rocks." *2nd Ed., Chapman & Hall.*

Findlay, J. D., Brooks, N.J., Mure, J .N., and Heron W. (1997). "Design of Axially Loaded Piles-United Kingdom Practice." *Design of Axially Loaded Piles-European Practice*, Eds. De Cock & Legrand, Balkema, Rotterdam.

Geotechnical Engineering Office (GEO) (1991). "Foundation Design of Caisson on Granitic and Volcanic Rocks." *GEO Report No. 8, Civil Engg. Department, Hong Kong.*

Geotechnical Engineering Office (GEO) (2006). "Foundation Design and Construction." *Geo Publ. 1/2006, Geotech. Engg. Office, Civil Engg. and Development Dept., Hong Kong.*

Ghosh D. K. and Srivastava, M. (1991). "Point-Load Strength: An Index for Classification of Rock Material." *Bull. of the Int. Assoc. of Engg. Geology*, 44, 27–33.

Gupton, C. and Logan, T. (1984). "Design Guidelines for Drilled Shafts in Weak Rocks of South Florida." *Proc. of the South Florida Annual ASCE Meeting*, Reston.

Horvath, R. G. and Kenney, T. C. (1979). "Shaft Resistance in Rock Socketed Drilled Piers." *Proc. of the Symp. on Deep Foundations*, ASCE, 182-214.

ISRM (1978a). "Suggested Methods for The Quantitative Description of Discontinuities in Rock Masses." *Int. J. of Rock Mech. and Mining Sci. & Geomech. Abst.*, 15(6), 319-368.

ISRM (1978b). "Suggested Methods for Determining Hardness and Abrasiveness of Rocks." *Int. J. of Rock Mech. and Mining Sci. & Geomech. Abst.*, 15(3), 89-98.

Jamshidi, A., Yazarloo, R., and Gheiji, S. (2018). "Comparative Evaluation of Schmidt Hammer Test Procedures for Prediction of Rock Strength." *Int. J. of Mining and Geo-Engg.*, 52(2), 199–206.

Kahraman, S. (2014). "The Determination of Uniaxial Compressive Strength from Point Load Strength for Pyroclastic Rock." *Engg. Geology*, 170, 33–42.

Kahraman, S., Fener, M., and Kozman, E. (2012). "Predicting the Compressive and Tensile Strength of Rocks from Indentation Hardness Index." *J. of the Southern African Inst. of Mining and Metallurgy*, 112(5), 331-339.

Kilic, A., and Teymen, A. (2008). "Determination of Mechanical Properties of Rocks Using Simple Methods." *Bull. of Engg. Geology and the Environ.*, 67, 237–244.

Kohno, M., and Maeda, H. (2012). "Relationship between Point Load Strength Index and Uniaxial Compressive Strength of Hydrothermally Altered Soft Rocks." *Int. J. of Rock Mech. and Mining Sci.*, 50, 147-157.

Krahenbuhl, J. K. and Wagner, A. (1983). "Survey, Design and Construction of Trail Suspension Bridges for Remote Area." *Vol. B, Swiss Centre for Technical Assistance, Switzerland.*

Kulhawy, F. H. (1978). "Geomechanical Model for Rock Foundation Settlement." *J. of Geotech. Engg.*, ASCE, 104(2), 211-227.

Kulhawy, F. H., and Goodman, R. E. (1980). "Design of Foundations on Discontinuous Rock." *Proc. of the Int. Conf. on Structural Foundations on Rock*, Sydney, Australia, 1, 209–220.

Kulhawy, F. H., and Jackson, C. S. (1989). "Some Observations on Undrained Side Resistance of Drilled Shafts." *Proc. Foundation Engg.: Current Principles and Practices*, ASCE, 2, 1011-1025.

Kulhawy, F. H. and Phoon, K. K. (1993). "Drilled Shaft Side Resistance in Clay Soil to Rock." *Proc. of the Conf. on Design and Performance of Deep Foundations: Piles and Piers in Soil and Soft Rock*, Reston, ASCE, 172-183.

Mehrotra, V. K. (1992). "Estimation of Engineering Properties of Rock Mass." *Ph. D. Thesis, IIT Roorkee, India.*

Meigh, A. C., and Wolski, W. (1979). "Design Parameters for Weak Rocks." *Proc. of the 7th European Conf. on Soil Mech. and Foundation Engg.*, Brighton, 5, 59–79.

Nam, M. S. (2004). "Improved Design for Drilled Shafts in Rock." *Ph.D. thesis, University of Houston, Houston, Tex.*

Nazir, R., Momeni, E., Jahed Armaghani, D., and Mohd Amin, M. F. (2013). "Correlation between Unconfined Compressive Strength and Indirect Tensile Strength of Limestone Rock Samples." *Electronics J. of Geotech. Engg.*, 18(I), 1737–1746.

NCHRP (2006). "Rock-Socketed Shafts for Highway Structure Foundations." *NCHRP Synthesis 360, Transportation Research Board, Washington.*

Neoh, C. A. (1998). "Design & Construction of Pile Foundation in Limestone Formation." *J. of Inst. of Engineers,* Malaysia, 59(1), 23-29.

Ng, C. W. W., Yau, T. L. Y., Li, J. H. M., and Tang, W. H. (2001). "Side Resistance of Large Diameter Bored Piles Socketed into Decomposed Rocks." *J. of Geotech. and Geoenviron. Engg.*, ASCE, 127(8), 642-657.

O'Neill, M. W. and Reese, L. C. (1999). "Drilled Shafts: Construction Procedures and Design Methods." FHWA-IF-99–025.

Peck, R. B., Hanson, W. E., and Thornburn, T. H. (1974). "Foundation Engineering." *2nd Ed., John Wiley and Sons.*

Prakoso, W. A. (2002). "Reliability-Based Design of Foundations in Rock Masses." *PhD Dissertation, Cornell University.*

Rahimi, M. R., Mohammadi, S. D., and Beydokhti, A. T. (2022). "Correlation between Schmidt Hammer Hardness, Strength Properties and Mineral Compositions of Sulfate Rocks." *Geotech. and Geological Engg.*, 40, 545-574.

Reese, L. C. and O'Neill, M. W. (1988). "Drilled Shafts: Construction Procedures and Design Methods." FHWA-HI-88-042.

Reynolds, R. T. and Kaderabek, T. J. (1980). "Miami Limestone Foundation Design and Construction." *New York,* ASCE, 859-872.

Rezazadeh, S. and Eslami, A. (2017). "Empirical Methods for Determining Shaft Bearing Capacity of Semi-Deep Foundations Socketed in Rocks." *J. of Rock Mech. and Geotech. Engg.*, 9, 1140-1151.

Rosenberg, P. and Journeaux, N. L. (1976). "Friction and End Bearing Tests on Bedrock for High Capacity Socket Design." *Canadian Geotech. J.*, 13(3), 324-333.

Rowe, R. K. and Armitage, H. H. (1984). "Design of Piles Socketed into Weak Rock." *Geotechnical research report, University of Western Ontario, Canada.*

Rowe, R. K. and Armitage, H. H. (1987). "A Design Method for Drilled Piers in Soft Rock." *Canadian Geotech. J.*, 24(1), 126-142.

Selcuk, L. and Yabalak, E. (2015). "Evaluation of the Ratio between Uniaxial Compressive Strength and Schmidt Hammer Rebound Number and Its Effectiveness in Predicting Rock Strength." *Nondestructive Testing and Evaluation*, 30(1), 1-12.

Singh, R. N., Hassani, F. P., and Elkington, P. A. S. (1983). "The Application of Strength and Deformation Index Testing to the Stability Assessment of Coal Measures Excavations." *24th U.S. Symp. on Rock Mech. (USRMS)*, Texas, 599-609.

Skempton, A. W. (1986). "Standard Penetration Test Procedures and the Effect in Sand of Overburden Pressure, Relative Density, Particle Size, Aging, And Overconsolidation." *Geotechnique*, 36(3), 425-447.

Stroud. M. (1974). "SPT in Insensitive Clays." *Proc. European Symp. on Penetration Testing*, 2.2, 367-375.

Taiyaqupt, M., Charusiri, P., and Ponsapich, W. (1986). "Geology and Stratigraphy of the Sri Racha area, Chonburi Province, Eastern Thailand." *Proc. GEOSEA V*, Geological Soc. of Malaysia, Bulletin 20, 2, 59-71.

Tandon, R. S. and Gupta, V. (2015). "Estimation of Strength Characteristics of Different Himalayan Rocks from Schmidt Hammer Rebound, Point Load Index, and Compressional Wave Velocity." *Bull. of Engg. Geology and the Environ.*, 74(2), 521–533.

Thorne, C. P. (1977). "The Allowable Loadings of Foundations on Shale and Sandstone in the Sidney Region." Part 3. Field test results. *Paper presented to Sydney Group of Australia Geomech. Soc., Inst. Engineers Australia.*

Toh, C. T., Ooi, T. A., Chiu, H. K., Chee, S. K., and Ting, W. N. (1989). "Design Parameters for Bored Piles in a Weathered Sedimentary Formation." *Proc. 12th Int. Conf. on Soil Mech. and Foundation Engg.,* Rio de Janeiro, 2, 1073–1078.

Vipulanandan, C., Hussain, A., and Usluogulari, O. (2007). "Parametric Study of Open Core-Hole on the Behavior of Drilled Shafts Socketed in Soft Rock." *Contemporary Issues in Deep Foundations: Proc. of Geo-Denver 2007,* Colo., Geotech. Special Pub. No. 158, Eds. Camp *et al.,* ASCE, Reston, Va., 1–10.

Waltham, A. C. (1994). "Foundations of Engineering Geology." *Chapman & Hall.*

Williams, A. F., Johnston, I. W., and Donald, I. B. (1980). "The Design of Socketed Piles in Weak Rock." *Proc. of the Int. Conf. on Structural Foundations on Rock,* Sydney, Australia, 327–347.

Zhang, L. (2004). "Drilled Shafts in Rock – Analysis and Design." *Balkema Publishers.*

Zhang, L. (2008). "Predicting the End Bearing Capacity of Rock Socketed Shafts." *Proc. of the 33rd Annual and 11th Int. Conf. on Piling and Deep Foundations, Deep Foundations Inst.*, 307–316.

Zhang, L. (2010). "Estimating the Strength of Jointed Rock Masses." *Rock Mech. and Rock Engg.*, 43(4), 391-402.

Zhang, L. and Einstein, H. H. (1998). "End Bearing Resistance of Drilled Shafts in Rock." *J. of Geotech. and Geoenviron. Engg.*, ASCE, 124(7), 574–584.